ELSEVIER

Chemistry and Physics of Lipids
86 (1997) 51–64

CPL
CHEMISTRY AND PHYSICS OF LIPIDS

Anisotropy and lifetime profiles for *n*-anthroyloxy fatty acids: a fluorescence method for the detection of bilayer interdigitation

R. Hutterer [a], F.W. Schneider [a], M. Hof [b,*]

[a] *Institute for Physical Chemistry, University of Würzburg, Marcusstrasse 9-11, D-97070 Würzburg, Germany*
[b] *Institute for Physical Chemistry, Charles University, Albertov 2030, Cz-12840 Prague 2, Czech Republic*

Received 9 October 1996; received in revised form 5 December 1996; accepted 30 December 1996

Abstract

A new fluorescence assay for the detection of interdigitated bilayer phases using the set of *n*-anthroyloxy stearic acids (*n*-AS, where $n = 2,3,6,9,12$) and 16-anthroyloxy palmitic acid (16-AP) is presented. Anisotropy measurements were performed for the *n*-AS dyes in multilamellar vesicles (MLV) composed of either 1,2-dimyristoyl-*sn*-glycero-3-phosphatidylcholine (DMPC), 1,2-dipalmitoyl-*sn*-glycero-3-phosphatidylcholine (DPPC), 1,2-dihexadecyl-*sn*-glycero-3-phosphatidylcholine (DHPC) or 1-stearoyl-2-lauroyl-*sn*-glycero-3-phosphatidylcholine (C18/12-diacylPC) with known gel phase structures. Plots of the steady-state anisotropy versus the position of the chromophore were obtained with characteristic shapes for non-interdigitated, mixed or fully interdigitated gel phases. Lifetime measurements revealed a somewhat smaller polarity gradient for the fully interdigitated DHPC compared to DPPC and extraordinarily long lifetimes for 16-AP in the mixed interdigitated C18/12-diacylPC which can be of diagnostic value for this specific gel phase structure. The assay was used for the investigation of the new asymmetric 1-stearyl-2-lauryl-*sn*-glycero-3-phosphatidylcholine (C18/12-dietherPC), providing evidence for a mixed interdigitated structure similar to that described previously for the corresponding C18/12-diacylPC. © 1997 Elsevier Science Ireland Ltd.

Keywords: Fluorescence Anisotropy; Bilayer interdigitation; Lifetime profiles; *n*-Anthroyloxy fatty acids: Diether lipids

1. Introduction

For a given composition of acyl chains in phospholipid molecules there is a tendency to maximize the van der Waals interactions in the acyl chain region while keeping the number of gauche rotamers per chain at a minimum. In addition, voids in the acyl chain region are energetically unfavourable. Another requirement for a stable packing is that the surface area provided by the lipid headgroup at the interface region and the

* Corresponding author. Fax: +420 2 6884818; e-mail: hof@troja.fjfi.cvut.cz.

PII S0009-3084(97)02659-5

cross sectional area provided by the acyl chains must match one another [1].

In the last few years it has been recognized that besides the classic bilayer arrangement another gel phase structure is possible in which the acyl chains of opposing monolayers interdigitate. Three types of bilayer interdigitation have been reported: fully interdigitated bilayers can occur in systems composed of lipids with either little or no chain asymmetry or in systems with the highest possible degree of asymmetry, including lysolipid species [1]. A wide variety of amphiphilic compounds has been reported to induce the interdigitated $L_{\beta}I$-phase in saturated like-chain phosphatidylcholines. Much work has been done on the induction of this phase by ethanol [2–8], but the $L_{\beta}I$-phase can also be adopted in presence of higher alcohols [9], benzyl alcohol, ethylene glycol [10–12], chlorpromacine [11], thiocyanate ions [12] and polymyxin B [13]. This interdigitated gel phase has also been observed in the absence of any inducer in DHPC [14–16] and 1,3-DPPC [17], as well as in DPPC and DSPC under hydrostatic pressure [18].

The second type, called mixed interdigitation, is less common and results when the difference between the *sn*-1 and *sn*-2 acyl chains (ΔC) is about half as long as the length of the longer acyl chain (CL), i.e. $\Delta C/CL \approx 0.5$ [10,19]. In calculating ΔC, the apparent length of the *sn*-2 chain in the gel state bilayer is taken to be 1.5 C–C bond lengths shorter than the total length of the chain in a nearly all-trans conformation [20], due to the abrupt *sn*-2 chain bend at the (C2) atom near the glycerol backbone region [21]. This mixed interdigitation is characterized by the long acyl chain extending completely across the bilayer whereas the two shorter chains meet end to end in the bilayer midplane.

Finally, a partial interdigitated bilayer packing mode exists in which the shorter chain from one monolayer pairs with the longer from the opposing monolayer. This arrangement has been proposed for medium asymmetric lipids like 1-stearoyl-2-myristoyl-*sn*-glycero-3-phosphatidylcholine [10,15,22] and for asymmetric lipids in the fluid crystalline phase [19,23,24].

For the detection of interdigitation X-ray diffraction [5,10–12,14,17,22,24,25] and neutron diffraction [18] are the most direct methods. However, infrared and Raman spectroscopy [26,27], electron spin resonance [28,29], differential scanning calorimetry (DSC) [3,14,15,30], NMR [31–33] and fluorescence spectroscopy [4,6,8,30] have also been used to detect and/or to study interdigitated lipid phases. A drawback of the diffraction methods is the large amount of material and the expensive facilities required. Fluorescence spectroscopy on the other hand has been widely used to study the structure and dynamics of model membranes due to its high sensitivity and short measurement times, at least for steady-state measurements. Yet, only few useful assays based on either pyrene [8] or DPH fluorescence [4] have been presented. The latter relies on intensity changes of DPH during a phase transition to the fully interdigitated phase and has the disadvantage that the $L_{\beta}I$-phase cannot be distinguished from other phases by DPH fluorescence alone [8]. While all these studies were concentrated on the EtOH-induced interdigitation of DPPC multilamellar vesicles, fluorescence has hardly been used to detect and study mixed interdigitated systems.

The *n*-anthroyloxy fatty acids (*n*-AS; $n =$ 2,3,6,9,12, 16-AP) constitute a unique set of fluorescent dyes with a common chromophore covalently attached at different positions along the acyl chain of the fatty acid. As the *n*-AS probes are known to insert into the membrane with the fatty acid chain parallel to the phospholipid acyl chains, their chromophore is located at a relatively defined depth in the bilayer, thus being able to detect polarity and fluidity gradients in a bilayer [34–36].

In this work we compare the fluorescence behaviour of the set of *n*-AS in both a lipid system showing full interdigitation (DHPC) and a system with mixed interdigitation (C18/12-diacyl PC) with corresponding non-interdigitating lipids (DPPC and DMPC, respectively) using steady-state anisotropy and lifetime measurements. Anisotropy profiles as a function of position of the chromophore are shown to be able to distinguish between the different bilayer arrangements in the

gel phase. 16-AP has been proven especially useful exhibiting extraordinary long lifetimes and large anisotropy values in the mixed interdigitated bilayer. Moreover, we characterize a new diether lipid (1-stearyl-2-lauryl-*sn*-glycero-3-phosphatidylcholine) and show that the described method can be used for the prediction of gel phase structures.

2. Materials and methods

1,2-Dimyristoyl-*sn*-glycero-3-phosphatidylcholine (DMPC), 1,2-dipalmitoyl-*sn*-glycero-3-phosphatidylcholine (DPPC) and 1,2-dihexadecyl-*sn*-glycero-3-phosphatidylcholine (DHPC) were obtained from FLUKA; 1-stearoyl-2-lauroyl-*sn*-glycero-3-phosphatidylcholine (C18/12-diacylPC) was from Avanti Polar Lipids. The new 1-stearyl-2-lauryl-*sn*-glycero-3-phosphatidylcholine (C18/12-dietherPC) was a generous gift of Dr. E. Grell. The set of *n*-anthroyloxy fatty acids (*n*-AS; $n = 2$, 3, 6, 9, 12 and 16-AP) was purchased from Molecular Probes.

The fluorophores were added to the respective lipid in $CHCl_3$ from an ethanolic stock solution to a final lipid/dye ratio of 200:1. The total lipid concentration was 1.0 mM for the time-resolved studies and 0.1 mM for steady-state anisotropy measurements.

The solvent was removed under a stream of N_2 and the remaining lipid/dye mixture was kept under vacuum overnight. Tris buffer (20 mM Tris, 100 mM NaCl, pH 7.5) containing 10% sucrose to prevent the sedimentation of the liposomes was added and the lipid film was allowed to swell for 1 h above the phase transition temperature with occasional vortexing to yield multilamellar vesicles (MLV). Small unilamellar vesicles (SUV) were prepared by sonication of the MLV suspension above the phase transition. The vesicles in the clear solution were allowed to anneal for 30 min and were centrifuged in order to remove MLV and titanium particles. Large unilamellar vesicles (LUV) were obtained by the extrusion method as described by MacDonald et al. [37]. The lipid/dye mixture was vortexed at a temperature above the phase transition and extruded through polycarbonate filters (Nucleopore, 100-nm pore size) using a LiposoFast extruder (Avestin).

The vesicle suspensions were kept at 5.0°C overnight to allow the formation of the respective interdigitated gel phases (DHPC, C18/12-diacylPC, C18/12-dietherPC) or non-interdigitated gel phases (DMPC, DPPC).

Fluorescence decays ($\lambda_{ex} = 358$ nm) were recorded at 430 nm with commercial single photon counting equipment (Edinburgh Instruments 199 S) and analyzed using an iterative reconvolution technique, as described [38]. The errors in the mean lifetimes given are ≤ 0.1 ns. Steady-state anisotropies were recorded with an Aminco Bowman II spectrometer using excitation and emission wavelength of 385 and 430 nm, respectively. Each data point represents an average value from six to eight single measurements; the maximal errors are ± 0.003. The temperature was controlled within 0.2°C.

3. Results

3.1. Steady-state anisotropy

Steady-state anisotropies as a function of temperature were recorded for the set of *n*-AS dyes and 16-AP in MLV composed of DPPC, DHPC, DMPC and C18/12-diacylPC, respectively. These results are summarized in Fig. 1. All dyes exhibit abrupt decreases of the steady-state anisotropies (r_{ss}) close to the respective temperature T_m of the chain melting transition ($P_{\beta'} \rightarrow L_\alpha$) for the symmetric diacyl lipids (DMPC ($T_m = 24$°C); DPPC ($T_m = 41$°C)), as described previously [35,36]. The change in anisotropy values is larger for those *n*-AS dyes which are localized more closely to the bilayer center (9-AS, 12-AS, 16-AP). While there is a clear fluidity gradient in the liquid crystalline phase (the r_{ss}-values decrease in the order $2 > 3 \approx 6 > 9 > 12 > 16$), the highest anisotropy in the gel phase was found for 6-AS. In the 'normal' gel phase structure as exhibited by DMPC and DPPC, 16-AP shows the lowest r_{ss}-values irrespective of temperature.

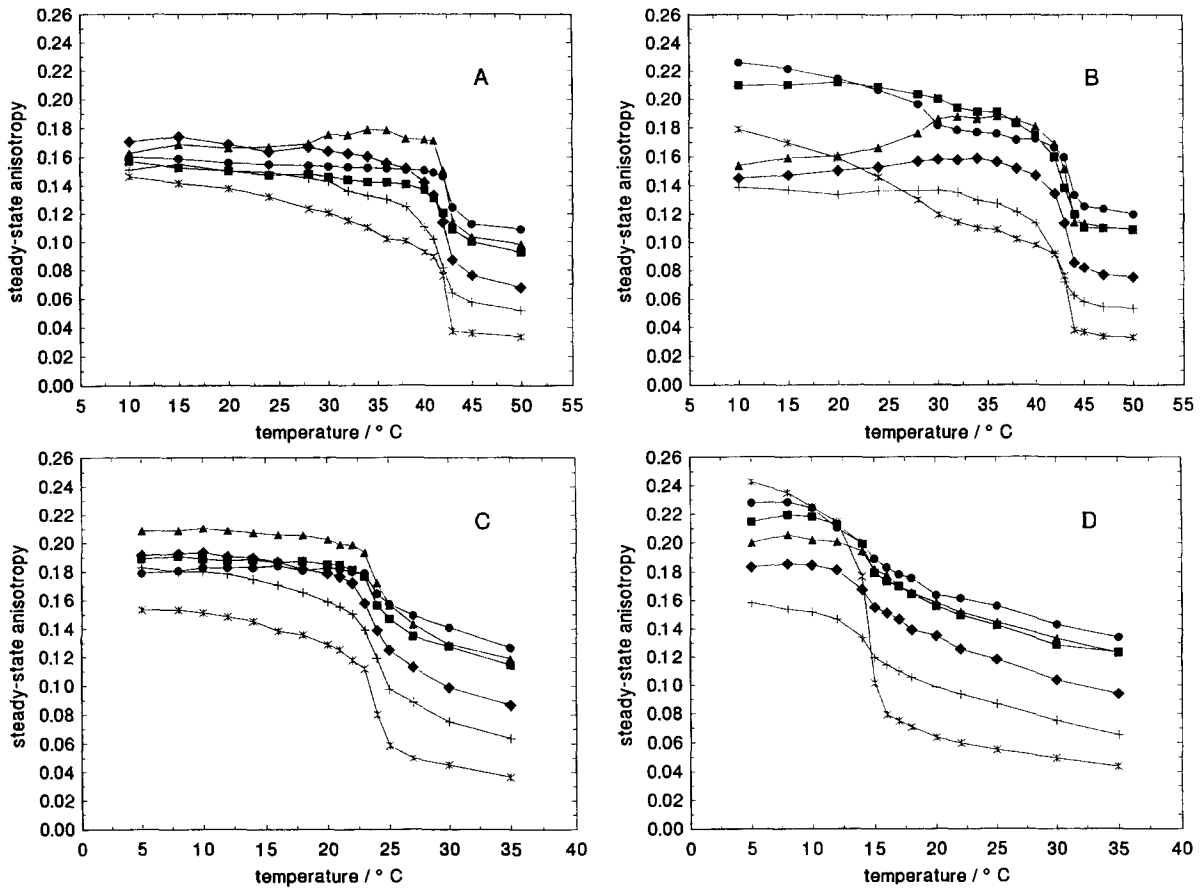

Fig. 1. Steady-state anisotropies of the set of *n*-AS dyes as a function of temperature in DPPC-MLV (A), DHPC-MLV (B), DMPC-MLV (C) and C18/12-diacylPC-MLV (D). The excitation wavelength was 385 nm, the emission was detected at 430 nm. Circles, 2-AS; boxes, 3-AS; triangles, 6-AS; diamonds, 9-AS; plus, 12-AS; stars, 16-AP.

A completely different behaviour has been observed for the asymmetric C18/12-diacylPC. At 5°C, a clear fluidity gradient is observed from 2-AS to 12-AS; however, 16-AP shows the highest steady-state anisotropy of all members (0.243), while in DMPC the lowest values (0.152) of all dyes was observed. At this temperature, C18/12-diacylPC is known to form a mixed interdigitated gel phase ($L_{\beta}I$) with three acyl chains per headgroup. The decrease of the r_{ss}-values for the *n*-AS dyes, associated with the transition to the liquid crystalline phase, is less sharp than in the non-interdigitated systems. However, 16-AP shows a very abrupt decrease in anisotropy from the highest value of all examined dyes below T_m to the lowest value above T_m. Considerably higher r_{ss}-values are observed for 2-AS in the interdigitated gel phase, suggesting higher membrane order in this region compared to the non-interdigitated phase (DMPC).

For DHPC, a fully interdigitated structure has been confirmed by X-ray and DSC [15], which converts to a normal gel phase at 34.5°C and to the liquid crystalline phase at 43.5°C. Compared to the non-interdigitated lipid DPPC, another characteristic temperature behaviour of the steady-state anisotropies of the set of *n*-AS dyes is observed. As in the mixed interdigitated phase, 2-AS shows high r_{ss}-values at low temperature ($r_{ss} = 0.232$ at 10°C) compared to the non-interdigitated phase in DPPC (0.161). Up to 30°C a continuous decrease of the anisotropy is observed,

followed by relatively constant values between 30°C and 40°C. A pronounced decrease occurs at the main phase transition temperature around 43°C. The behaviour of 3-AS is quite similar. For 6-AS, however, there is an increase of the anisotropy with increasing temperature up to around 32°C, followed by nearly constant values up to 40°C and a sharp decrease at the main transition. For 9-AS and 12-AS only minor changes in the anisotropy occur between 10°C and 40°C, with a sharp decrease again at the phase transition. 16-AP is more restricted in the fully interdigitated phase at 10°C compared to the normal gel phase in DPPC, but there is a fast and continuous decrease of the r_{ss}-values up to the main phase transition, where the anisotropy drops to very low values, as observed in the other examined lipids.

The data described above have been used to construct profiles of the steady-state anisotropy versus the position of the chromophore along the acyl chain for some characteristic temperatures. In Fig. 2 these profiles are compared both for the non-interdigitated (DMPC) and the mixed interdigitated (C18/12-diacylPC) (A) and the non-interdigitated (DPPC) and the fully interdigitated lipid (DHPC) (B), respectively. Plots are shown for both lipids of a pair at the same reduced temperatures relative to the main transition temperature T_m. The non-interdigitated gel phases are characterized by a rise of the anisotropy from position 2 to 6, followed by a steady decrease of r_{ss}. Above T_m, 2-AS exhibits the highest r_{ss}-values. A pronounced fluidity gradient from position 2 to 16 is characteristic for the liquid crystalline phase of all investigated lipids. The mixed interdigitated phase is characterized by higher anisotropies for 2-AS and 3-AS and a continuous decrease down to position 12. The most intriguing feature, however, are the extraordinary high anisotropy values for 16-AP in the mixed interdigitated phase, which are much higher than in a 'normal' ($\underline{\Delta}$ non-interdigitated) gel phase.

A similar profile is observed for the fully interdigitated phase at low temperatures (10°C). Again, the r_{ss}-values are high for 2- and 3-AS, while considerably lower for 6-, 9-, and 12-AS. In contrast to the non-interdigitated phase (DPPC), a considerable rise of r_{ss} is observed from 12-AS to 16-AP. This profile changes markedly at higher temperatures. At 32°C the maximal anisotropy is observed for 3-AS, followed by 6-AS and a continuous decrease from 6-AS to 16-AP. Above T_m, the profile is similar to those of the other lipids.

Thus, each of the three examined gel phase types (non-interdigitated, mixed interdigitated, fully interdigitated) yields a different characteristic profile which seems to be of diagnostic value

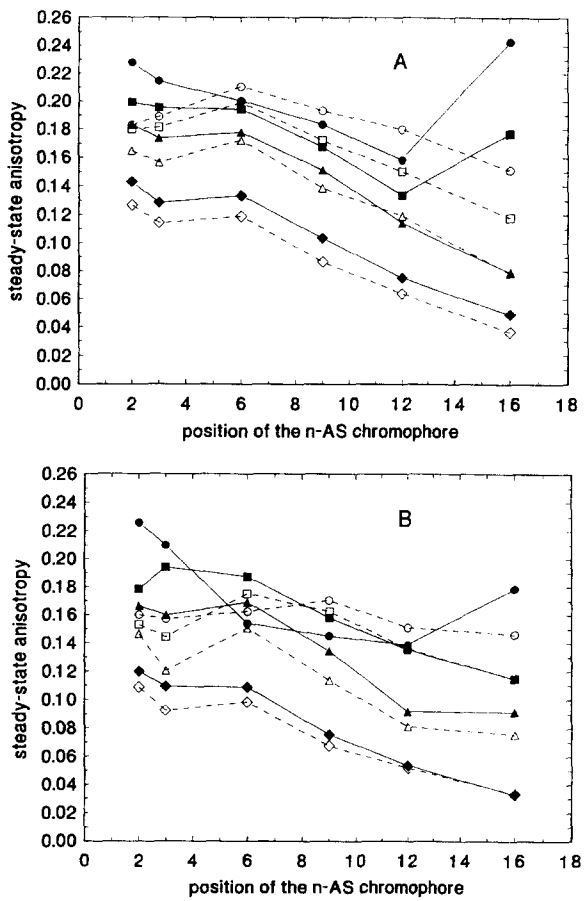

Fig. 2. Steady-state anisotropy profiles of the n-AS dyes in DMPC-MLV (open symbols) and C18/12-diacylPC-MLV (filled symbols) (A) and in DPPC-MLV (open symbols) and DHPC-MLV (filled symbols) (B), respectively. Plots are shown for the same reduced temperatures relative to the phase transition. (A) Filled symbols: 5°C (circles), 14°C (boxes), 18°C (triangles), and 30°C (diamonds); open symbols: 10°C (circles), 19°C (boxes), 23°C (triangles), and 35°C (diamonds). (B) Filled and open symbols: 10°C (circles), 32°C (boxes), 42°C (triangles) and 50°C (diamonds).

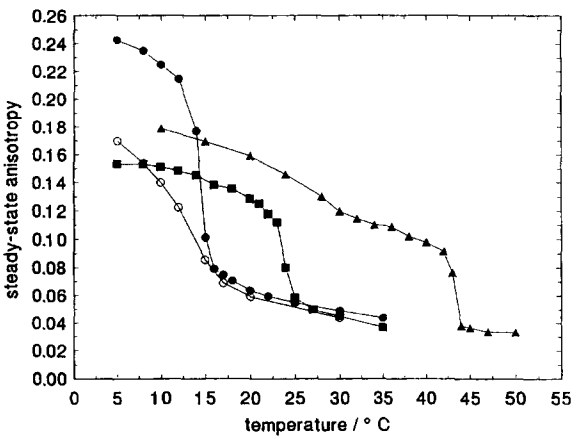

Fig. 3. Steady-state anisotropies as a function of temperature of 16-AP in C18/12-diacylPC-MLV (filled circles), C18/12-diacylPC-SUV (open circles), DHPC-MLV (triangles) and DMPC-MLV (boxes). The excitation wavelength was 385 nm, the emission was detected at 430 nm.

for the determination of the packing type of a specific lipid. Within this set of probes, 16-AP is clearly the most useful and interesting one. Its extreme different behaviour in DMPC, DHPC and C18/12-diacylPC has been summarized in Fig. 3. Very high anisotropies are observed in the mixed interdigitated phase in both multilamellar and large unilamellar vesicles (LUV-data not shown). In contrast, considerably smaller values were observed in small unilamellar vesicles, indicating that formation of a mixed interdigitated phase is not possible in small vesicles due to geometrical constraints.

Steady-state measurements were done for another system which is known to exhibit interdigitation, i.e. the induction of a fully interdigitated phase of DPPC by EtOH. This system has been investigated by several groups [2–8] and a fluorescent assay based on steady-state fluorescence intensities has been shown to monitor the transition from the non-interdigitated to the fully interdigitated phase in DPPC [4]. We were able to reproduce the decrease in steady-state intensity of 1,6-diphenyl-1,3,5-hexatriene (DPH) at an EtOH concentration between 1.0 and 1.2 M as described by Nambi et al. [4] and found that the steady-state anisotropy of DPH is also sensitive to the EtOH induced interdigitation; however, the decrease is less sharp (not shown).

The r_{ss}-data at 20°C for the set of n-AS dyes versus the ethanol concentration (A) and the corresponding anisotropy profiles for four representative EtOH concentrations (B) are shown in Fig. 4. In the absence of EtOH the highest r_{ss}-value was obtained for 6-AS, with decreasing values down to 16-AP. No major changes in this behaviour up to 1.0 M EtOH were found. However, there is a pronounced change between 1.0 and 1.4 M EtOH which is exactly the concentration range

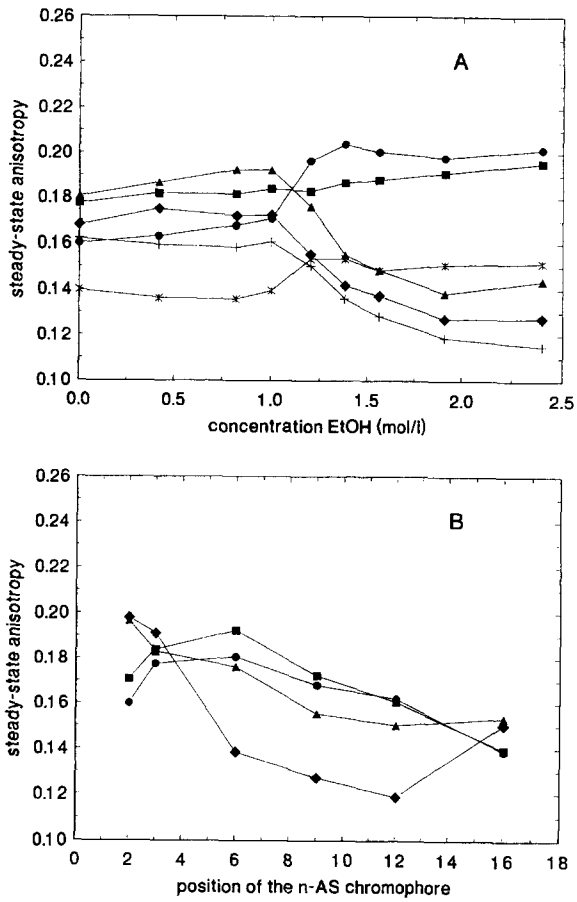

Fig. 4. Steady-state anisotropies of the n-AS dyes in DPPC-MLV at different EtOH-concentrations. (A) Plots of the steady-state anisotropy as a function of the EtOH-concentration. The excitation wavelength was 385 nm, the emission was detected at 430 nm. The temperature was 20°C. Circles, 2-AS; boxes, 3-AS; triangles, 6-AS; diamonds, 9-AS; plus, 12-AS; stars, 16-AP. (B) Anisotropy profiles of the n-AS dyes in DPPC-MLV for different EtOH-concentrations: circles, 0 mol/l; boxes, 1.0 mol/l; triangles, 1.2 mol/l; diamonds, 1.9 mol/l EtOH.

in which the transition to the fully interdigitated phase of DPPC was reported to occur [4,5]. While a strong increase of r_{ss} was observed for 2-AS and 16-AP, 3-AS was hardly effected by the increase of the EtOH concentration from 1.0 to 1.4 M. For 6-, 9- and 12-AS the r_{ss}-values decreased considerably during this phase transition. A further increase in the EtOH concentration to 1.9 M leaves the anisotropies of 2-AS and 16-AP quite unaffected, while they decrease further for 6-, 9- and 12-AS. The anisotropy profile obtained at 1.9 M EtOH (Fig. 4B) is typical for a fully interdigitated phase, as may be seen by comparison with the profile for DHPC at 10°C (Fig. 2B). High r_{ss}-values are found for 2- and 3-AS. The anisotropy drops markedly for 6-, 9- and 12-AS but increases again going to 16-AP. While the absolute r_{ss}-values for the n-AS are somewhat lower in the EtOH-induced fully interdigitated phase than in the interdigitated phase of DHPC at low temperature, the shapes of the profiles are very similar, providing strong support for the use of such profiles in determining gel phase structures.

3.2. Decay time measurements

Previous studies have postulated a lower polarity gradient for interdigitated bilayers [29]. As the lifetimes of the set of n-AS dyes are sensitive to polarity [34–36], decay time measurements were performed with the n-AS probes in non-interdigitated, mixed interdigitated and fully interdigitated bilayers.

In a recent study we have clarified the fluorescence decay behaviour of the n-AS dyes in membranes. We have shown that besides the intramolecular relaxation process postulated earlier [39] solvent relaxation significantly contributes to the overall relaxation behaviour. However, the fluorescence decay at 430 nm appears to be a good indicator for the polarity gradient within the bilayer [40]. It is described by a biexponential decay for all dyes. The mean decay times, calculated according to

$$\langle \tau \rangle = \frac{(a_1 \tau_1^2 + a_2 \tau_2^2)}{(a_1 \tau_1 + a_2 \tau_2)}$$

where a_1 and a_2 are the pre-exponential factors of both components given in Table 1 for some representative temperatures. They increase from 2-AS to 16-AP in a normal bilayer system like DPPC. The mean lifetime of 2-AS was taken as 100% and the decay times of the other n-AS dyes were expressed as percentual increase (or decrease) relative to 2-AS. This procedure yields a characteristic profile for the decay behaviour in different bilayer arrangements, shown in Fig. 5A. Four different temperatures below and above the phase transition were examined. Considerably larger increases of the mean decay times of the n-AS with increasing depth of incorporation were observed for the non-interdigitated DPPC. For example, the mean decay time for 16-AP at 20°C was only 25% higher in DHPC compared to 37% in DPPC. At 32°C the respective values are 37 and 52%. This behaviour seems to be consistent with a fully interdigitated structure with smaller bilayer thickness compared to the non-interdigitated gel phase. Thus, 16-AP, being localized close to the center of the bilayer in DPPC, will adopt a position closer to the headgroup region in the fully interdigitated DHPC. There it senses a more polar environment, leading to a shorter decay time. In contrast, the decay time of 2-AS was about 0.4 ns longer in DHPC (20°C), presumably due to a somewhat lower polarity in this membrane region caused by the terminal methyl groups in the interdigitated structure.

The relative increase of the decay times of the n-AS relative to 2-AS remains larger in DPPC than in DHPC at higher temperatures, although the fully interdigitated gel phase of DHPC converts to a normal gel phase above 34.5°C, suggesting that a somewhat smaller polarity gradient is retained in DHPC compared to DPPC. The reason for the decrease in decay times for 6- and 9-AS (relative to 2-AS) at low temperatures is not clear and will not be considered further.

Comparative decay time measurements were also performed for the n-AS in MLV composed of DMPC and in C18/12-diacylPC. The pattern for DMPC (Fig. 5B) shows some unexpected differences compared to that observed in DPPC (Fig. 5A). An increase of the mean decay time of 16-AP was observed from 5°C to 25°C; only

Table 1
Mean fluorescence lifetimes of the set of AS-dyes for selected temperatures in unsymmetric and symmetric diacyl- and diether lipids (the standard errors are ± 0.1 ns).

Lipid	Temp. (°C)	⟨τ⟩/ns				
		2-AS	6-AS	9-AS	12-AS	16-AP
DAPC	5	9.1	10.1	9.9	11.4	16.2
	13	8.1	9.5	10.7	12.0	15.9
	15	7.7	9.3	10.7	12.1	15.0
	17	7.6	9.1	10.7	11.9	13.4
	25	6.9	8.4	10.1	11.7	12.6
DMPC	10	8.9	10.1	10.5	12.3	10.4
	18	7.8	9.5	10.5	12.0	11.7
	20	7.6	9.3	10.4	12.1	11.6
	22	7.5	9.2	10.5	12.0	11.8
	30	6.4	8.0	10.1	11.7	12.4
DHPC	20	8.8	8.0	7.4	8.4	11.1
	32	7.5	7.6	7.9	8.6	10.3
	42	5.9	6.9	8.2	8.8	9.9
	50	4.5	5.2	7.3	8.1	8.3
DPPC	20	8.4	8.7	9.0	10.3	11.6
	32	7.1	8.1	8.6	9.9	11.0
	42	5.9	7.4	9.2	10.2	10.5
	50	4.7	5.9	7.9	9.2	9.5

above this temperature, ⟨τ⟩ decreases, as expected. All other *n*-AS dyes showed a continuous decrease of ⟨τ⟩ with increasing temperature. Thus, at 5°C there is a larger percentual increase in the mean decay times from 2-AS to 12-AS (+39%) which drops to 18% for 16-AP. At higher temperatures the percentual increases for 12-AS and 16-AP are quite similar.

In contrast, a unique behaviour of 16-AP in C18/12-diacylPC has been observed. The decay behaviour is close to monoexponential with an extreme long decay time of about 17 ns in the gel phase contributing more than 90% to the total fluorescence intensity. Such a long decay component for 16-AP has not been observed in any other vesicle system studied by us up to now [40].

Above 15°C, 16-AP shows an abrupt decrease of the decay time (from 15.0 ns at 15°C to 13.4 ns at 17°C; Table 1) and further to 12.5 ns at 25°C which is very similar to that in DMPC at the same reduced temperature (12.4 ns). Thus, the transition from the mixed interdigitated to the liquid crystalline state is accompanied by a drastic change of the environment of 16-AP. Above the main transition, the relative increases of the decay times of the *n*-AS relative to 2-AS at the same reduced temperature are quite similar for DMPC and C18/12-diacylPC, suggesting an essentially equal structure for the liquid crystalline phase.

3.3. C18/12-dietherPC—a new lipid with mixed interdigitated gel phase?

While the gel phase structure for the C18/12-diacylPC is well known from X-ray diffraction data, nothing is known about the structure of the corresponding diether-PC. In a recent publication [41] we have compared the solvent relaxation behaviour of polarity sensitive probes in the C18/12-diacyl- and C18/12-dietherPC and found essential differences in the headgroup organization of both lipids.

For the gel phase a mixed interdigitated structure similar to that found for the C18/12-diacylPC

may be expected. Therefore, we investigated the steady-state anisotropy and the decay behaviour for the set of *n*-AS in MLV composed of this new asymmetric diether-PC which exhibits a main phase transition at 18–19°C, as measured by DSC (Dr. E. Grell, private communication). As with C18/12-diacylPC, a very high r_{ss}-value was obtained for 2-AS at the lowest temperature (5.0°C), with decreasing values in the series $3 \approx 6 > 9 > 12$-AS (Fig. 6). From 12-AS to 16-AP an increase in r_{ss} of ≈ 0.03 was detected. Although this increase

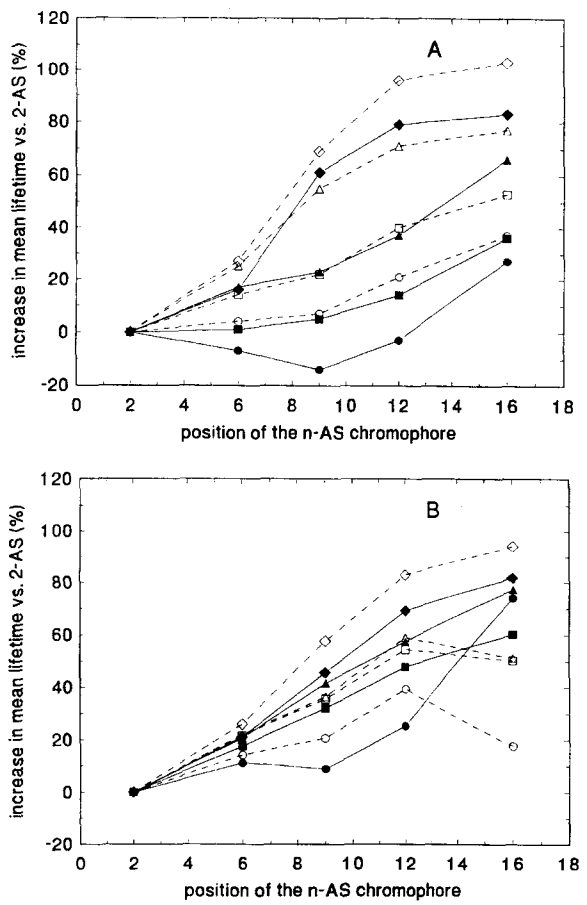

Fig. 5. Percentual increases of the mean lifetimes of 6-, 9- and 12-AS and 16-AP relative to 2-AS. The excitation wavelength was 358 nm, the emission was detected at 430 nm. (A) Open symbols: DPPC-MLV; filled symbols: DHPC-MLV; circles, 20°C; boxes, 32°C; triangles, 42°C; diamonds, 50°C. (B) Open symbols: DMPC-MLV; circles, 10°C; boxes, 18°C; triangles, 22°C; diamonds, 30°C; filled symbols, C18/12-diacylPC-MLV; circles, 5°C; boxes, 13°C; triangles, 17°C; diamonds, 25°C.

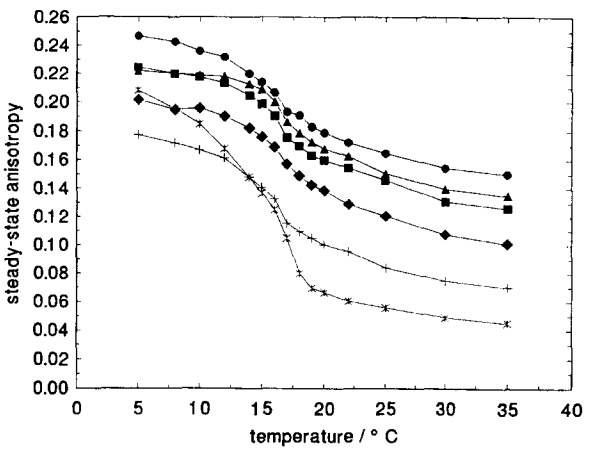

Fig. 6. Steady-state anisotropies of the set of *n*-AS dyes as a function of temperature in C18/12-dietherPC-MLV. The excitation wavelength was 385 nm, the emission was detected at 430 nm. Circles, 2-AS; boxes, 3-AS; triangles, 6-AS; diamonds, 9-AS; plus, 12-AS; stars, 16-AP.

is not as pronounced as in the case of the C18/12-diacylPC, it seems to be indicative for an interdigitated structure. The behaviour of 16-AP is between that observed in the mixed interdigitated C18/12-diacylPC with a very high gel phase value and a sharp decrease near the phase transition and that in fully interdigitated DHPC with somewhat lower values at deep temperature and a continuous decrease up to the transition from the fully interdigitated to the normal rippled gel phase.

Similar to C18/12-diacylPC the decay time measurements yield a uniquely long decay time for 16-AP at temperatures below the phase transition which drops to values similar to those for 16-AP in the other lipid systems above the phase transition (Fig. 7).

4. Discussion

Interdigitated membrane structures have attracted considerable interest during the last 10 years both due to their unique structural properties and their implication for membrane function. Although most information has been probably obtained by X-ray diffraction and NMR-techniques the search for new, less material and time

consuming assays to identify interdigitation has continued. In a recent study of Zeng and Chong [42] the extreme polarity sensitivity of Prodan (6-propionyl-2-(dimethylamino)naphthalene) has been used to detect the formation of the $L_{\beta}I$-phase in DPPC bilayers. While the emission spectra of the set of *n*-AS dyes also shift with increasing solvent polarity, they exhibit considerably smaller shifts in response to a lipid phase transition compared to Prodan. In addition, the large shifts observed by Zeng and Chong for Prodan are at least in part due to Prodan molecules which have been expelled from the lipid phase during interdigitation. The AS dyes, in contrast, are fixed much more tightly in the membrane than Prodan and thus do not leave the bilayer during interdigitation. Therefore, large spectral shifts of the *n*-AS due to bilayer interdigitation are not expected.

In this work we have examined the steady-state anisotropy and decay behaviour of the set of *n*-AS in different lipid systems which are known to exhibit either non-interdigitated, mixed or fully interdigitated gel phases. Each of these gel phase types has been shown to yield a characteristic

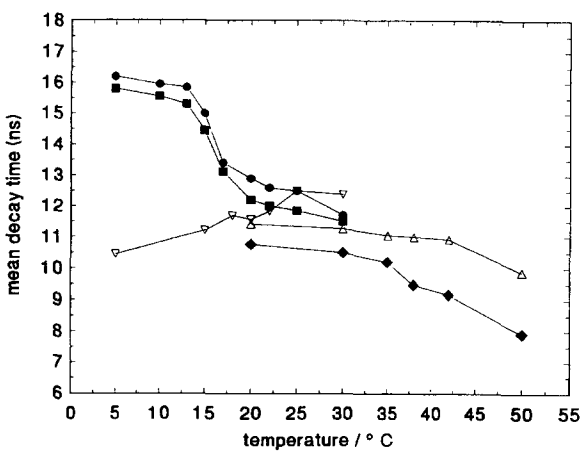

Fig. 7. Mean fluorescence decay times of 16-AP as a function of temperature in lipids adopting different gel phase types. The excitation wavelength was 358 nm, the emission was detected at 430 nm. Circles, C18/12-diacylPC-MLV (mixed interdigitated); boxes, C18/12-dietherPC-MLV (mixed interdigitated); diamonds, DHPC-MLV (fully interdigitated); triangles up, DPPC-MLV (non-interdigitated); triangles down, DMPC-MLV (non-interdigitated).

anisotropy profile as a function of position of the chromophore. The main phase transition is detected by all probes, producing a sharp decrease of the r_{ss}-values. This decrease is larger for those *n*-AS which are closer to the bilayer center of the non-interdigitated bilayers (DMPC, DPPC). Thus, while in the gel phase the fluidity gradient is small due to the ordered acyl chain packing, a much larger fluidity gradient is observed in the fluid phase. With increasing distance from the glycerol backbone the number of gauche conformations of the acyl chains increase leading to very low order near the methyl terminus. The fluid phase behaviour of all investigated systems is very similar, with a pronounced fluidity gradient and very low anisotropy values for 16-AP.

In contrast, quite different anisotropy profiles have been observed for the different gel phases. The most important features are the higher r_{ss}-values of 2-AS for both the mixed and fully interdigitated phases and the unique behaviour of 16-AP in the mixed interdigitated bilayer. The fluorescence anisotropy of the *n*-AS probes is a function of both the resistance to depolarizing rotations and the orientational constraint imposed by the anisotropic environment [43]. Moreover, the motion of the aromatic ring is the result of at least two different modes of rotation. The out-of-plane mode, excitable at 316 nm, results from rotation of the aromatic ring around the ester linkage, while the in-plane mode depends on the reorientation of the acyl chain. Both modes of depolarization contribute at an excitation wavelength of 358 nm. Time-resolved anisotropy measurements have shown that the in-plane motion is hindered in the gel phase [43], i.e. the anisotropy values do not decrease to zero even after long times but to a finite value r_{∞}. Due to this complications a full interpretation of the anisotropy behaviour on the basis of steady-state data is not possible. Rather we wish to point out the use of the anisotropy profiles, especially the behaviour of 16-AP as a 'fingerprint' for the corresponding structure, i.e. as a simple means to differentiate between a non-, mixed- and fully interdigitated structure. Obviously, the steady-state anisotropies depend also on the fluorescence lifetimes, as a longer lifetime will give the fluorophor more time for depolariza-

tion. However, as we have shown for 16-AP, this dye exhibits the highest steady-state anisotropy in the mixed interdigitated phase, although a uniquely long lifetime is observed for this system. Thus, we may be sure that the observed effects in the steady-state anisotropy are not due to differences in the fluorescence lifetimes but are closely related to the lipid structure in the interdigitated bilayers.

The higher r_{ss}-values for 2-AS and 3-AS in both types of interdigitated gel phases were not surprising as it has been shown by DSC [19,44] and Raman spectroscopy [27] that mixed interdigitated structures are highly ordered, even more ordered than the gel state of the corresponding non-interdigitated symmetric diacyl-PC of same molecular weight.

In the case of 2- and 3-AS the proximity of the terminal bulky methyl group may lead to a hindered motion of the chromophore, resulting in high r_{ss}-values. The higher anisotropies of 6- and 9-AS in the mixed compared to the fully interdigitated gel phase could be also related to the influence of the apposing methyl groups in the center of the mixed interdigitated phase which is absent in the fully interdigitated phase. While 16-AP will be localized close to the center of non-interdigitated bilayers which is the region of lowest order it will be positioned closer to the glycerol backbone and the terminal methyl group of a lipid of the opposing monolayer in the fully interdigitated structure. This creates a region of lower flexibility compared to its position in the normal bilayer at low temperatures, yielding higher r_{ss}-values. However, there is a considerable decrease in anisotropy even within the gel phase suggesting either some gain in flexibility of the region where 16-AP resides which is not sensed by the other probes, or a special temperature sensitive mode of depolarization due to the attachment of the chromophore at the terminal of the acyl chain. A unique behaviour of 16-AP has been observed in the mixed interdigitated structure at low temperature, with very high r_{ss}- and lifetime values. We have no obvious explanation for the origin of the observed long lifetime in the gel phase of C18/12-diacylPC. Due to the reduced bilayer thickness of the interdigitated phase compared to DMPC the 16-AP chromophore should be localized close to the lipid/water interface, sensing an environment of considerable polarity if an all-trans conformation for the palmitoyl chain is assumed. As the decay times for the *n*-AS decrease with increasing polarity, a much shorter decay time than observed experimentally would be expected. One possible explanation is that 16-AP loops back into the bilayer in order to avoid the exposure of the hydrophobic aromatic ring to the polar lipid/water interface. This may allow a position in a highly restricted environment where little quenching occurs and which seems not to be favoured in a fully interdigitated gel phase. Although the reason for the long lifetime of 16-AP observed in the mixed interdigitated gel phase will still have to be elucidated, this dye seems to be a useful tool for the identification of this peculiar lipid arrangement.

A comparison of the decay time profiles of the non-interdigitated DPPC and the fully interdigitated DHPC reflect the concept of the less steep dielectric constant gradient for an interdigitated gel phase compared to a non-interdigitated one, due to the difference in bilayer thickness [24]. The increases of the mean decay time relative to 2-AS are smaller for the fully interdigitated DHPC than for DPPC.

Steady-state anisotropy profiles have also been obtained for the set of *n*-AS in the system DPPC/EtOH which is known to undergo a transition from the non-interdigitated to a fully interdigitated gel phase at 20°C and an EtOH concentration of 1.0–1.2 M [4,5]. The transition to the fully interdigitated phase is clearly accompanied by a pronounced change of the anisotropy profiles when the EtOH concentration is increased from 1.0 to 1.4 M. Due to interdigitation 2-AS and 16-AP are placed in a more rigid environment compared to the normal gel phase, while 6-, 9- and 12-AS become less restricted. This is the same behaviour as observed for the fully interdigitated phase of DHPC at low temperatures. The strong similarity of the anisotropy profiles for the fully interdigitated DHPC and the EtOH-induced interdigitated phase of DPPC support the view that the shape of the profile can be used to detect interdigitated gel phases.

We used this approach based on the steady-state anisotropy and lifetime profiles to derive some information on the gel phase structure of the new asymmetric C18/12-dietherPC. Although the steady-state anisotropy values for 16-AP do not reach the high values obtained for the corresponding C18/12-diacylPC at low temperature the increase in r_{ss} from 12-AS to 16-AP as well as the high values for 2- and 3-AS may be regarded as a clear hint for an interdigitated structure. Much lower steady-state anisotropies were observed for 2-AS and 16-AP in non-interdigitated gel phase structures than in DHPC (fully interdigitated), C18/12-diacylPC (mixed interdigitated) and the new C18/12-dietherPC.

While a clear differentiation between a mixed and a fully interdigitated gel phase for C18/12-diether-PC based on steady-state anisotropy alone seems difficult, the mean lifetimes for 16-AP give a clear indication in favour of a mixed interdigitated structure. Mean lifetimes between 12.0 and 13.0 ns were typically observed for 16-AP in non-interdigitated gel phase bilayers. In DHPC, even shorter lifetimes (around 11.0 ns) were obtained. Thus, mean decay times above 15.0 ns as found for both C18/12-diacylPC and the corresponding diether-PC (Fig. 7) are unique and seem to be associated with a mixed interdigitated bilayer. Of course, while these data cannot prove the existence of a mixed interdigitated phase for C18/12-dietherPC, they show the usefulness of our approach for obtaining information concerning the gel phase structure of new lipid systems which have not yet been examined by X-ray analysis. Of course, the results presented in this work are representative only for saturated phosphatidylcholines; unsaturated PC-analogues exhibit very low phase transition temperatures (gel → liquid crystalline) and to our knowledge, nothing is known about formation of interdigitated gel phases by unsaturated lipid species.

Our fluorescence approach for the detection of interdigitated lipid structures may be compared with the fluorescence assay developed by Nambi et al. (1988) [4]. These authors used the fluorescence intensity of DPH in DPPC which shows an abrupt decrease when the EtOH concentration is sufficient to induce the formation of the fully interdigitated phase. One drawback of this assay is the fact that only a transition from one gel phase to another can be monitored by a change of the intensity but no information is available on the type of gel phase which had been present before the transition. In contrast, an anisotropy profile with the set of *n*-AS recorded for any specific phase may be able to decide between interdigitated and non-interdigitated phases without taking the sample through a phase transition. Adding the information which may be gained from lifetime measurements with 16-AP, even more insight into the type of interdigitation may be obtained due to the unique long lifetime of 16-AP in mixed interdigitated bilayers.

5. Conclusion

Although X-ray diffraction techniques will remain indispensable for the unambiguous determination of lipid phase structures the present work shows that considerable information can be obtained by relatively simple anisotropy measurements, especially, if additional decay time measurements are performed.

The set of *n*-AS dyes yields characteristic anisotropy profiles for non-interdigitated, mixed and fully interdigitated bilayers, as shown for DMPC, DPPC, C18/12-diacylPC, DHPC and DPPC in the presence of EtOH. The shape of these plots of the steady-state anisotropy versus the position of the chromophore can be used to predict the gel phase structure of new lipid species, as exemplified in this work for the new C18/12-dietherPC. 16-AP turned out to be an especially useful probe due to its high anisotropy and its uniquely long lifetime in mixed interdigitated structures. Because absolute values of steady-state anisotropy and lifetimes characteristic for different types of gel phase structures may be obtained, the present fluorescence assay seems to be superior to an older fluorescence approach [4] based on a change of relative fluorescence intensities of DPH upon bilayer interdigitation.

References

[1] Slater, J.L. and Huang, C. (1988) Interdigitated bilayer membranes. Prog. Lipid Res. 27, 325–359.

[2] Rowe, E.S. (1992) in Alcohol: Neurobiology and Physiology Watson, R. (Ed.), CRC Press, Boca Raton, FL, pp. 239–267.

[3] Rowe, E.S. and Cutrera, T.A. (1990) Differential scanning calorimetric studies of alcohol interactions with distearoylphosphatidylcholine: transition to the interdigitated phase. Biochemistry 29, 10398–10404.

[4] Nambi, P., Rowe, E.S. and McIntosh, T.J. (1988) Studies of the ethanol-induced interdigitated gel phase in phosphatidylcholines using the fluorophore 1,6-diphenyl-1,3,5-hexatriene. Biochemistry 27, 9175–9182.

[5] Simon, S.A. and McIntosh, T.J. (1984) Interdigitated hydrocarbon chain packing causes the biphasic transition behaviour in lipid/alcohol suspensions. Biochim. Biophys. Acta 773, 169–172.

[6] Komatsu, H. and Rowe, E.S. (1991) Effect of cholesterol on the ethanol-induced interdigitated gel phase in phosphatidylcholine: use of fluorophore pyrene-labeled phosphatidylcholine. Biochemistry 30, 2463–2470.

[7] Zeng, J., Smith, K.E. and Chong, P.L-G. (1993) Effects of alcohol-induced lipid interdigitation on proton permeability in L-α-dipalmitoylphosphatidylcholine vesicles. Biophys. J. 65, 1404–1414.

[8] Yamazaki, M., Miyazu, M. and Asano, T. (1992) Studies of alcohol-induced interdigitated gel phase in phosphatidylcholine multilamellar vesicles by the excimer method. Biochim. Biophys. Acta 1106, 94–98.

[9] Rowe, E.S. and Campion, J.M. (1994) Alcohol induction of interdigitation in distearoylphosphatidylcholine: fluorescence studies of alcohol chain length requirements. Biophys. J. 67, 1888–1895.

[10] McDaniel, R.V., McIntosh, T.J. and Simon, S.A. (1983) Nonelectrolyte substitution for water in phosphatidylcholine bilayers. Biochim. Biophys. Acta 731, 97–108.

[11] McIntosh, T.J., McDaniel, R.V. and Simon, S.A. (1983) Induction of an interdigitated gel phase in fully hydrated phosphatidylcholine bilayers. Biochim. Biophys. Acta 731, 109–114.

[12] Cunningham, B.A. and Lis, L.J. (1986) Thiocyanate and bromide ions influence the bilayer structural parameters of phosphatidylcholine bilayers. Biochim. Biophys. Acta 861, 237–242.

[13] Theretz, A., Ranck, J.L. and Tocanne, J.F. (1983) Polymyxin B-induced phase separation and acyl chain interdigitation in phosphatidylcholine/phosphatidylglycerol mixtures. Biochim. Biophys. Acta 732, 499–508.

[14] Ruocco, M.J., Siminovitch, D.J. and Griffin, R.G. (1985) Comparative study of the gel phases of ether- and ester-linked phosphatidylcholines. Biochemistry 24, 2406–2411.

[15] Laggner, P., Lohner, K., Degovics, G., Müller, K. and Schuster, A. (1987) Structure and thermodynamics of the dihexadecylphosphatidylcholine-water system. Chem. Phys. Lipids 44, 31–60.

[16] Kim, J.T., Mattay, J. and Shipley, G.G. (1987) Gel phase polymorphism in ether-linked dihexadecylphosphatidylcholine bilayer. Biochemistry 26, 6592–6598.

[17] Serrallach, E.N., Dijkman, R., De Haas, G.H. and Shipley, G.G. (1983) Structure and thermotropic properties of 1,3-dipalmitoylglycero-2-phosphate. J. Mol. Biol. 170, 155–174.

[18] Braganza, L.F. and Worcester, D.L. (1986) Hydrostatic pressure induces hydrocarbon chain interdigitation in single-component phospholipid bilayers. Biochemistry 25, 2591–2596.

[19] Xu, H. and Huang, C. (1987) Scanning calorimetric study of fully hydrated asymmetric phosphatidylcholines with one acyl chain twice as long as the other. Biochemistry 26, 1036–1043.

[20] Mason, J.T. and Huang, C. (1981) Lipids 16, 604–608.

[21] Zaccai, G., Büldt, G., Seelig, G. and Seelig, J. (1979) Neutron diffraction studies on phosphatidylcholine model membranes. J. Mol. Biol. 134, 673–706.

[22] Mattai, J., Sripada, P.K. and Shipley, G.G. (1987) Mixed-chain phosphatidylcholine bilayers: structure and properties. Biochemistry 26, 3287–3297.

[23] McIntosh, T.J., Simon, S.A., Ellington, Jr., J.C. and Porter, N.A. (1984) New structural model for mixed-chain phosphatidylcholine bilayers. Biochemistry 23, 4038–4044.

[24] Hui, S.W., Mason, J.T. and Huang, C. (1984) Acyl chain interdigitation in saturated mixed-chain phosphatidylcholine bilayer dispersions. Biochemistry 23, 5570–5577.

[25] Ranck, J.L. and Tocanne, J.F. (1982) Polymyxin induces interdigitation in dipalmitoylglycerol lamellar phase with stiff hydrocarbon chains. FEBS Lett. 143, 175–177.

[26] O'Leary, T.J. and Levine, I.W. (1984) Raman spectroscopic study of an interdigitated lipid bilayer dipalmitoylphosphatidylcholine dispersed in glycerol. Biochim. Biophys. Acta. 776, 185–189.

[27] Huang, C., Mason, J.T. and Levin, I.W. (1983) Raman spectroscopic study of saturated mixed-chain phosphatidylcholine multilamellar dispersions. Biochemistry 22, 2775–2780.

[28] Boggs, J.M., Rangaraj, G. and Watts, A. (1989) Behaviour of spin labels in a varity of interdigitated lipid bilayers. Biophys. Biochim. Acta 981, 243–253.

[29] Boggs, J.M. and Rangaraj, G. (1985) Phase transitions and fatty acid spin label behaviour in interdigitated lipid phases induced by glycerol and polymyxin. Biochim. Biophys. Acta 816, 221–233.

[30] Kao, Y.L., Chong, P.L.-G. and Huang, C. (1990) Dynamic motions of 1,6-diphenyl-1,3,5-hexatriene in interdigitated C(18):C(10)phosphatidylcholine bilayers. Biophys. J. 58, 947–956.

[31] Ruocco, M.J., Makriyannis, A., Siminovitch, D.J. and Griffin, R.G. (1985) Deuterium NMR investigation of ether- and ester-linked phosphatidylcholine bilayers. Biochemistry 24, 4844–4851.

[32] Frenzell, J., Arnold, K. and Nuhn, P. (1978) Calorimetric, ^{13}C NMR, and ^{31}P NMR studies of the interaction of

some phenothiazin derivatives with dipalmitoylphosphatidylcholine model membranes. Biochim. Biophys. Acta 507, 185–197.

[33] Siminovitch, D.J., Jeffrey, K.R. and Eibl, H. (1983) A comparison of the headgroup conformation and dynamics in synthetic analogues of dipalmitoylphosphatidylcholine. Biochim. Biophys. Acta 727, 122–134.

[34] Thulborn, K.R. and Sawyer, W.H. (1978) Properties and the locations of a set of fluorescent probes sensitive to the fluidity gradient of the lipid bilayer. Biochim. Biophys. Acta 511, 125–140.

[35] Thulborn, K.R., Tilley, L.M., Sawyer, W.H. and Treolar, F.E. (1979) The use of *n*-(9-anthroyloxy) fatty acids to determine fluidity and polarity gradients in phospholipid bilayers. Biochim. Biophys. Acta 558, 166–172.

[36] Hutterer, R., Lanig, H., Schneider, F.W. and Hof, M. (1997) Solvent relaxation behaviour of *n*-anthroyloxy fatty acids in PC-vesicles and paraffin oil: a time-resolved emission spectra study. Biochim. Biophys. Acta 1323, 195–207.

[37] MacDonald, R.C., MacDonald, R.I., Menco, B.Ph., Takeshita, K., Subarao, N.K. and Hu, L. (1991) Small volume extrusion apparatus for preparation of large unilamellar vesicles. Biochim. Biophys. Acta 1061, 297–303.

[38] Hof, M., Schleicher, J. and Schneider, F.W. (1989) Time resolved fluorescence in doped aerogels and organosilicate glasses. Ber. Bunsenges. Phys. Chemie 93, 1377–1381.

[39] Matayoshi, E.D. and Kleinfeld, A.M. (1981) Emission wavelength-dependent decay of 9-anthroyloxy fatty acid membrane probes. Biophys. J. 35, 215–235.

[40] Brand, K. (1993) Ph.D. Theses, University of Würzburg.

[41] Hutterer, R., Schneider, F.W., Fidler, V., Grell, E. and Hof, M. (1996) Time-evolved emission spectra of Prodan and Patman in large unilamellar vesicles: a comparison between diether- and diacyllipids. J. Fluorescence, in press.

[42] Zeng, J. and Chong, P.L.-G. (1991) Interactions between pressure and ethanol on the formation of interdigitated DPPC Liposomes: a study with Prodan fluorescence. Biochemistry 30, 9485–9491.

[43] Kawato, S., Kinosita, K. and Ikegami, A. (1977) Dynamic structure of lipid bilayers studied by nanosecond fluorescence techniques. Biochemistry 16, 2319–2324.

[44] Mason, J.T., Huang, C. and Biltonen, R.L. (1981) Calorimetric investigations of saturated mixed-chain phosphatidylcholine bilayer dispersions. Biochemistry 20, 6086–6092.